JOURNAL OF MATERIALS SCIENCE 33 (1998) 3303–3311

Dynamic fracture of a functionally gradient material having discrete property variation

VENKITANARAYANAN PARAMESWARAN, ARUN SHUKLA
Dynamic Photomechanics Laboratory, Department of Mechanical Engineering and Applied Mechanics, University of Rhode Island, Kingston, RI – 02881, USA
E-mail: shuklaa@egr.uri.edu

A functionally gradient material (FGM) with discrete property variation is prepared, and the dynamic fracture in this material is studied using the technique of photoelasticity combined with high-speed photography. Transparent sheets required for the study are made by casting a polyester resin mixed with varying amounts of plasticizer. The mechanical (quasi-static and dynamic) and optical properties of the material are evaluated as a function of the plasticizer content. Results of material characterization show that the fracture toughness increases with increasing plasticizer content, whereas the Young's modulus decreases. The material fringe constant and the dynamic modulus are observed to be relatively insensitive to plasticizer content. The FGM is then prepared by casting together thin strips having different plasticizer content. The dynamic crack propagation phenomenon is studied for four different property variations along the crack propagation direction, and the effects of these property variations on crack speed, crack jump distance and dynamic stress intensity factor are investigated. Results of this investigation show that increasing the toughness in the direction of crack growth reduces the crack jump distance as compared to an increasing-decreasing toughness variation for the same initial energy.

1. Introduction

The advent of functionally gradient materials (FGMs) in which the properties vary progressively in a given direction calls for investigation into the fracture oriented failure of such materials. These materials usually have two constituents with the composition varying spatially from one end to the other. The fracture toughness in such FGMs varies along the thickness, and hence, the effect of this variation on the dynamic crack propagation needs to be studied. The property variation in FGMs can be either continuous or piece-wise continuous (i.e stepped). Analytical solutions for crack-tip stress fields and stress intensity factors in FGMs subjected to static loads are given by Erdogan [1] and Batra and Jin [2]. However, dynamic fracture studies in FGMs are scarce and have received little attention.

This paper describes the investigations carried out on dynamic fracture of FGMs using the technique of photoelasticity combined with high-speed photography. A method for fabricating an FGM suitable for photoelastic studies using polyester resin and plasticizer is described. The property variation in the material was achieved by changing the amount of plasticizer. The mechanical and optical properties of the material were evaluated for plasticizer contents varying from 0% to 50% in steps of 10%. An FGM in which the properties vary in a piecewise continuous manner was fabricated by casting together thin strips having different plasticizer content. Four different property variations, namely increasing toughness, decreasing toughness, increasing-decreasing toughness and decreasing-increasing toughness, were considered in this study. Dynamic fracture of these FGMs was studied using the modified compact tension (MCT) specimen geometry, and the effects of the variation of toughness on crack speed, crack jump distance and the dynamic stress intensity factor were analysed. Fractographic studies were also carried out to observe the fracture surface features and the results are presented.

2. Material preparation and characterization

The technique of photoelasticity requires that the specimens be made of transparent and birefringent material. The first objective of this study was to prepare an FGM which would be suitable for photoelastic studies. Commercially available materials are homogeneous and hence cannot be used for this kind of study. This necessitated in-house preparation of the material. General purpose polyester resin MR 17090 (supplied by Ashland Chemical Company), when cast into sheets, exhibits properties suitable for photoelastic studies. The mechanical properties of these sheets

0022–2461

can be varied by adding another resin, MR 9600 (a plasticizer supplied by the same manufacturer), in varying proportions during the casting process. These resins are available in liquid form, have the same mass density and can be mixed to obtain a homogenous mixture. The curing process can be initiated by adding suitable amounts of a catalyst and an accelerator. In this study, 0.85% by weight of methyl ethyl ketone peroxide and 0.03% by weight of cobalt octoate were used as the catalyst and accelerator, respectively.

2.1. Casting procedure

The polyester resin and plasticizer in the required proportions, along with the catalyst and accelerator, were mixed thoroughly and poured into a half-inch thick mould. The walls of the mould were lined with thin (0.18 mm) mylar sheets to obtain a clear flat surface. The resin mixture was allowed to cure in the mould at 21 °C for 48 h. The sheets were then removed from the mould and post cured in an air circulating oven for 4 h at 52 °C followed by 5 h at 63 °C. After machining to the required size, these sheets were annealed at 80 °C for 6 h to relieve any residual stresses induced during machining. This procedure consistently produced sheets which were clear, transparent and free of residual stresses.

2.2. Variation of properties with plasticizer content

The mechanical properties such as Young's modulus, shear modulus, Poisson's ratio and fracture toughness were evaluated for plasticizer content varying from 0 to 50% in steps of 10%. The fracture toughness was determined using the single edged notched (SEN) specimen geometry whereas the Young's modulus and Poisson's ratio were determined using standard test procedures.

The variation of the quasi-static mechanical properties with plasticizer content is shown in Fig. 1. It was observed that addition of plasticizer resulted in sheets which were tougher and more flexible. Increasing the plasticizer content from 0% to 50% resulted in a 45% decrease in the quasi-static Young's modulus of the material, as can be seen from Fig. 1a, and the decrease was non-linear in nature. The Poisson's ratio of the material registered a 30% increase as the plasticizer was increased from 0 to 50% and the variation was non-linear, as can be observed from Fig. 1b. This indicates that the material behaviour tends to be more incompressible in nature as the plasticizer content is increased. The shear modulus, which is a function of the Young's modulus and Poisson's ratio, decreased by about 50%.

The variation of fracture toughness with plasticizer content is shown in Fig. 2. As can be seen from Fig. 2, the fracture toughness increased by about 60% as the plasticizer content was varied from 0 to 50%. This may be due to the fact that a reduction in Young's modulus leads to reduced yield strength of the material resulting in larger plastic deformation at the crack tip. The variation of the mechanical properties became

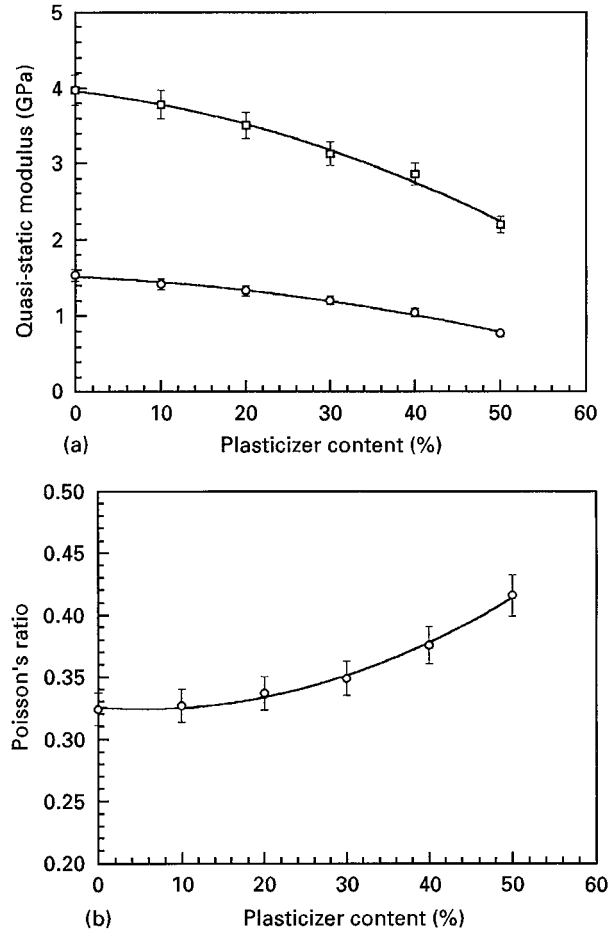

Figure 1 Mechanical properties of polyester-plasticizer sheets for various compositions. ((□) Young's and (○) shear modulus in (a)).

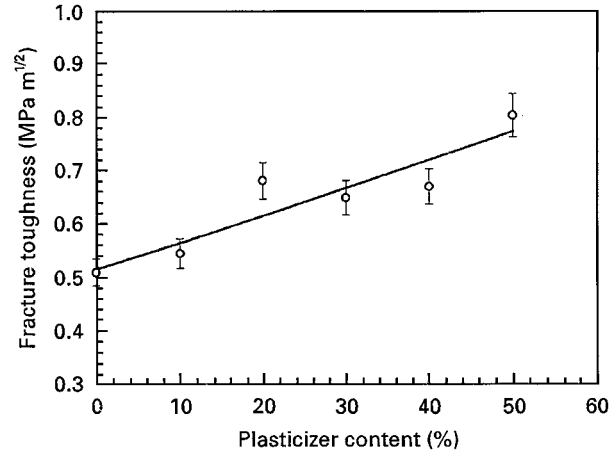

Figure 2 Fracture toughness of polyester-plasticizer sheets for various compositions.

increasingly sensitive at higher plasticizer content as can be observed from the nature of the curves in Fig. 1. Table I summarizes the properties of the material.

The material fringe constant was determined through photoelastic experiments [3] and the variation was observed to be small (Fig. 3), and hence can

TABLE I Properties of polyester-plasticizer sheets

% Plasticizer	Fracture toughness (MPa $m^{1/2}$)	Young's modulus (GPa)	Poisson's ratio	Fringe constant (kN(m-fringe)$^{-1}$)	Shear modulus (GPa)
0	0.51	3.98	0.32	35.3	1.53
10	0.55	3.79	0.33	33.7	1.41
20	0.68	3.51	0.34	33.6	1.32
30	0.65	3.14	0.35	32.1	1.20
40	0.67	2.87	0.38	33.8	1.04
50	0.80	2.20	0.42	31.8	0.78

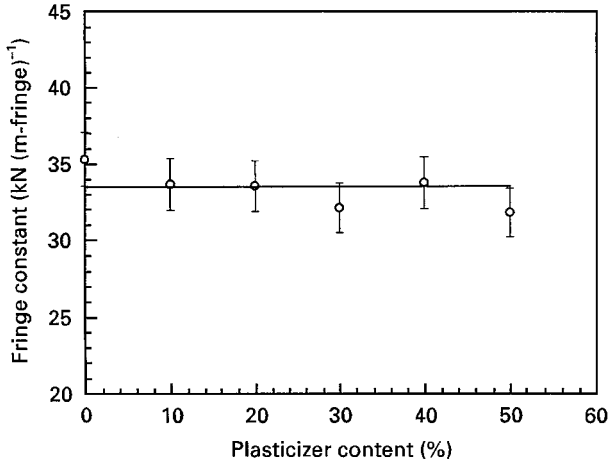

Figure 3 Material fringe constant of polyester-plasticizer sheets for various compositions.

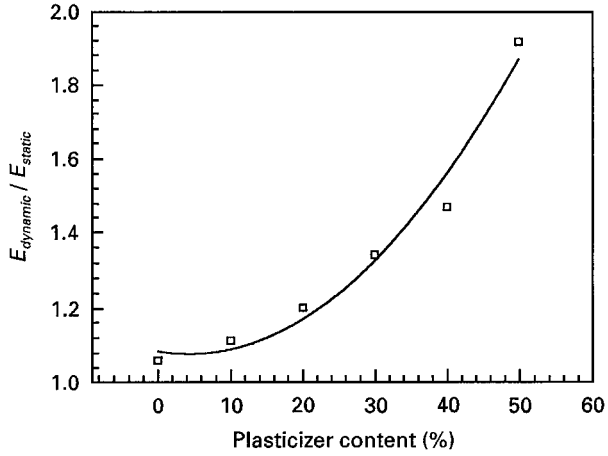

Figure 4 Change in rate sensitivity of polyester-plasticizer sheets for various compositions. (E–Young's modulus).

be regarded as constant. In order to determine the dynamic properties, a half-plane made of the material was loaded by detonating an explosive on the free surface. The explosion sets up dilatational and distortional waves in the specimen. The resulting isochromatic fringe patterns were photographed, and the location of the wave fronts was obtained as a function of time. The wave speeds in the material were estimated from this information, and the dynamic Young's modulus and the shear modulus were calculated using these wave speeds [4]. The dynamic properties showed no variation as the plasticizer content was increased. However, the ratio of the dynamic modulus to the quasi-static modulus increased by 80% with plasticizer increasing from 0 to 50%, as shown in Fig. 4. This implies that the material becomes more rate sensitive with increasing plasticizer content. The dynamic properties of the material are given in Table II. Since the material fringe constant remains constant and other mechanical properties vary with plasticizer content, this material system is an ideal candidate for making FGMs suitable for photoelastic studies. Even though a procedure for making an FGM with continuous variation in properties is not evolved, an FGM with stepped variation in properties can be easily made by casting together thin strips having varying plasticizer content. By changing the thickness and plasticizer content of the strips, different property profiles can be achieved.

TABLE II Dynamic properties of polyester-plasticizer sheets

Dilatational wave speed, c_1 (m s^{-1})	2160
Shear wave speed, c_1 (m s^{-1})	1200
Young's modulus, E (GPa)	4.5
Shear modulus, μ (GPa)	1.7
Poisson's ratio	0.32
Mass density, ρ (kg m^{-3})	1180

3. Dynamic fracture experiments

3.1. Specimen geometry and fabrication

The second objective of this study was to investigate the effects of the property variations on dynamic crack propagation in FGMs. The modified compact tension (MCT) specimen geometry used in this study is shown in Fig. 5. The specimens were made by bonding together 13 mm-wide strips having different plasticizer content. These strips were machined to have square edges, and the bonding faces were sanded to obtain a better bond. The strips were then bonded by casting a very thin layer (125 μm) of polyester-plasticizer mixture. The plasticizer content of the bonding mixture was equal to that of the strip having higher plasticizer content, e.g. a 20% plasticizer strip was bonded to a 30% plasticizer strip with a 30% plasticizer mix. After bonding, the specimen was cured at 21 °C for 48 h and postcured at 38 °C for 2 h.

FGMs having four different property variations were prepared by varying the plasticizer content of the strips. The percentage variation of plasticizer content in these four FGMs were 0 to 50, 50–0, 0–50–0, and 50–0–50, in steps of 10%. These variations in plasticizer content resulted in FGMs having increasing toughness, decreasing toughness, increasing-decreasing toughness and decreasing-increasing toughness in the direction of crack growth, respectively. Fig. 6 shows the variation of the shear modulus and fracture toughness along the direction of crack propagation in these specimens. The MCT specimen had a starter notch of length 76 mm. The notch tip was blunted to facilitate loading of the specimen beyond the static toughness of the material.

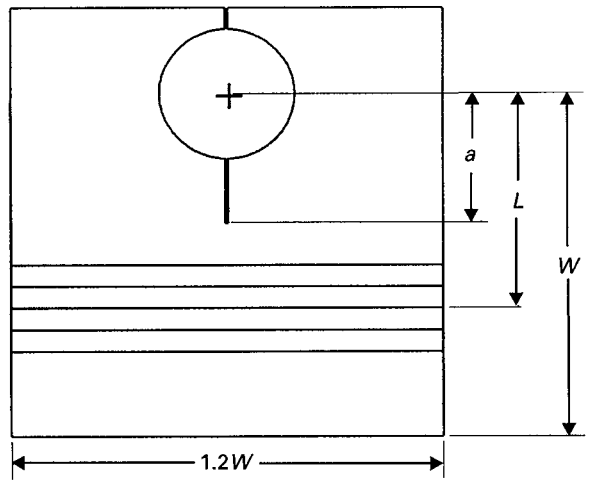

Figure 5 Modified compact tension (MCT) specimen geometry. (W = 200 mm, a = 76 mm, thickness = 13 mm).

3.2. Experimental procedure

A series of six experiments was performed to investigate the effect of the toughness variation along the direction of crack growth on dynamic crack propagation. The specimens were loaded to the predetermined load values using a specially designed loading frame placed on the optical bench of a high-speed camera as shown in Fig. 7. The crack was initiated by pulling a sharp knife across the crack tip. As the crack began to propagate, it cut a thin line of silver conducting paint, which triggered a multiple spark Cranz-Schardin camera to take twenty pictures of the propagating

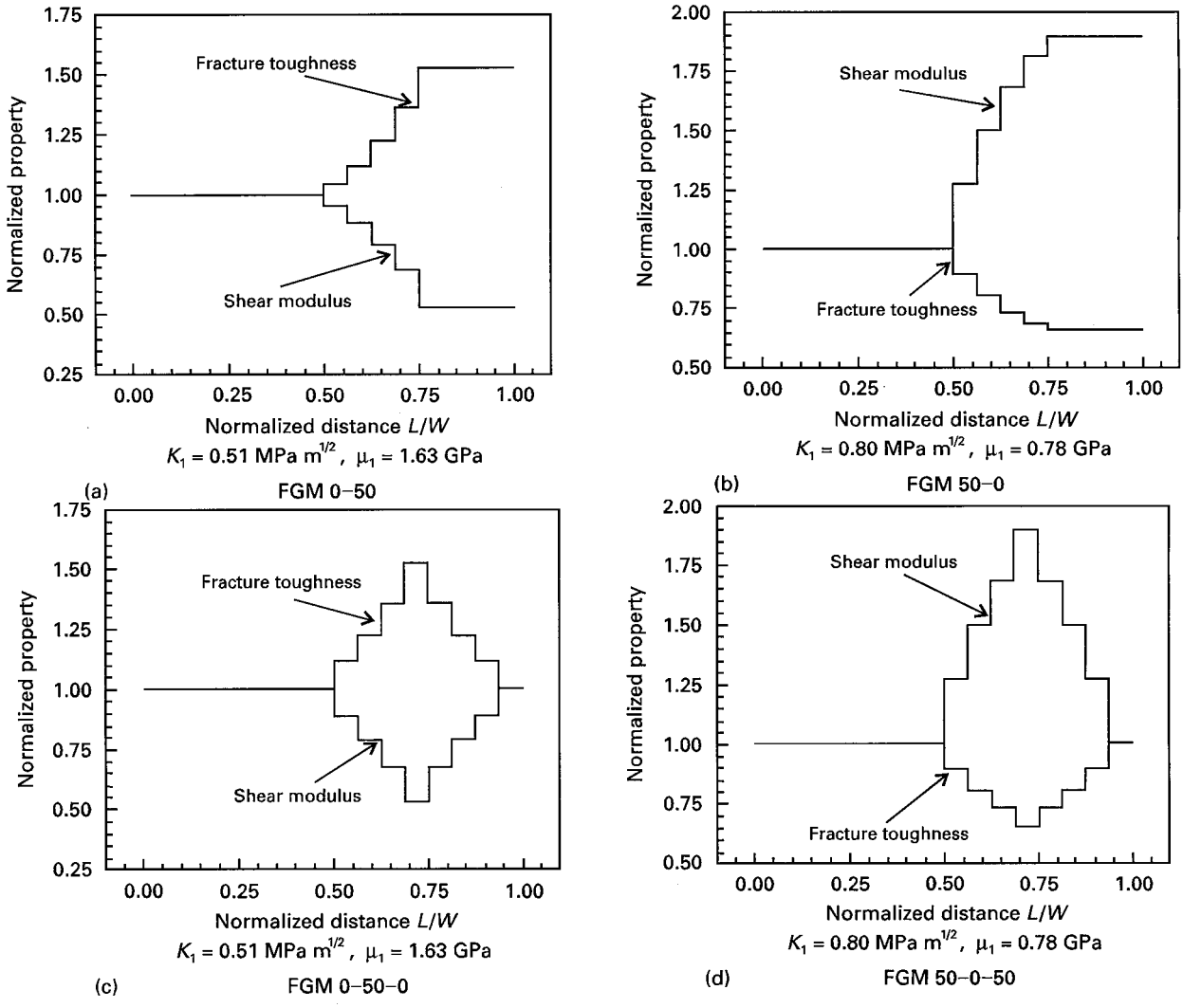

Figure 6 Property variation along the specimen width for the four different FGMs considered in this study. Properties are normalized with respect to their corresponding value of the first layer K_1 (fracture toughness) and μ_1 (shear modulus).

crack at preselected time intervals. The first set of ten photographs was taken at a framing rate of 200 000 frames s^{-1}, whereas, the next set of ten was taken at a framing rate of 40 000 frames s^{-1}.

In order to compare the effects of the toughness variation on dynamic fracture, the experiments were conducted under identical initial conditions. The initiation stress intensity factor (K_Q) and initial strain energy in the specimen are two parameters which influence dynamic crack propagation. In two of these experiments, the ratio of the initiation stress intensity factor to the static initiation toughness, K_Q/K_{IC}, (K_{IC} – toughness of the strip containing the starter notch) was held constant, and the effect of increasing toughness and decreasing toughness on dynamic crack propagation was studied. However, in these experiments, the initial energy present in the specimen was different. The K_Q values and the corresponding strain energy in the specimen are given in Table III. It can be seen that the strain energy in the 50–0 FGM is three times larger than that of the 0–50 FGM for the same K_Q/K_{IC} ratio. In the remaining four experiments, the initial strain energy in the specimen was held constant, and the effect of the four different toughness variations on dynamic crack propagation was studied. In order to determine the initial strain energy in the specimens, compliance calibration of these specimens was carried out by measuring the load point displacement for different load values. The strain energy for a given load was obtained by integrating the load-displacement curve.

3.3. Analysis of experimental data

The location of the crack tip was determined from the photographs for different instants of time, and the crack speed was calculated from this information. The crack jump distance was obtained from the post-mortem analysis of the fractured specimen. The dynamic stress field around a steadily moving crack tip can be represented as a singular series [5], in which the coefficient of the first term is proportional to the dynamic stress intensity factor K_D. The stress field around a crack tip exhibits an inverse square root singularity for homogeneous materials and interface cracks. It has been shown by Erdogan [1] that the same is true for the case of FGMs, if the properties vary in a continuous manner. In the present study, the variation in properties was piece-wise continuous, and hence, the strength of the crack-tip singularity at the interface may be different. The power of the crack-tip singularity at the interface, was shown to be a function of the material constants, and Cook and Erdogan [6] provide the functional relation for static loading as

$$2\alpha\cos(\pi\lambda) - (\beta\lambda^2 + \gamma) = 0 \tag{1}$$

$$\alpha = (m + \kappa_2)(1 + m\kappa_1), \quad \beta = -4(m + \kappa_2)(1 - m),$$

$$\gamma = (1 - m)(m + \kappa_2) + (1 + m\kappa_1)(m + \kappa_2) - m(1 + \kappa_1)(1 + m\kappa_1)$$

$$m = \frac{\mu_2}{\mu_1}$$

$$\kappa_{1,2} = \frac{3 - \nu_{1,2}}{1 + \nu_{1,2}} \text{ for generalized plane stress}$$

where μ_1 and μ_2 are the shear modulii, ν_1 and ν_2 the Poisson's ratio of the two materials involved and $(1 - \lambda)$ is the power of the singular term. The deviation of the power of the singular term from $-1/2$ at the interfaces between strips having different plasticizer content is shown in Fig. 8. It is evident from Fig. 8 that the maximum deviation of the power of the singular term is 5% for a quasi-static case and occur for a 40–50 interface. Hence, the deviation of the power of singularity is ignored, and the crack-tip stress fields are assumed to be similar to that in a homogeneous material.

The isochromatic fringe patterns obtained form the photographs represent contours of constant maximum shear stress and are related to the fringe order through the stress-optic law.

$$\sigma_1 - \sigma_2 = \frac{Nf_\sigma}{h} \tag{2}$$

where σ_1 and σ_2 are the principal stresses, N the fringe order, h the specimen thickness and f_σ is the material

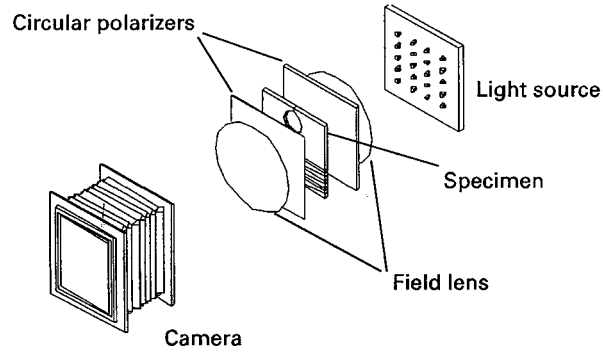

Figure 7 Schematic of the experimental setup used for dynamic fracture studies.

TABLE III Summary of results of dynamic experiments

Specimen configuration	Load (N)	K_Q (MPa $m^{1/2}$)	K_Q/K_{IC}	Energy (J)	Crack jump distance (mm)
0–50	680	0.83	1.6	0.14	53.4
50–0	1060	1.32	1.6	0.42	127.0
0–50	1000	1.25	2.4	0.32	95.3
0–50–0	1000	1.25	2.4	0.32	114.0
50–0	800	1.00	1.2	0.32	76.2
50–0–50	800	1.00	1.2	0.32	76.2

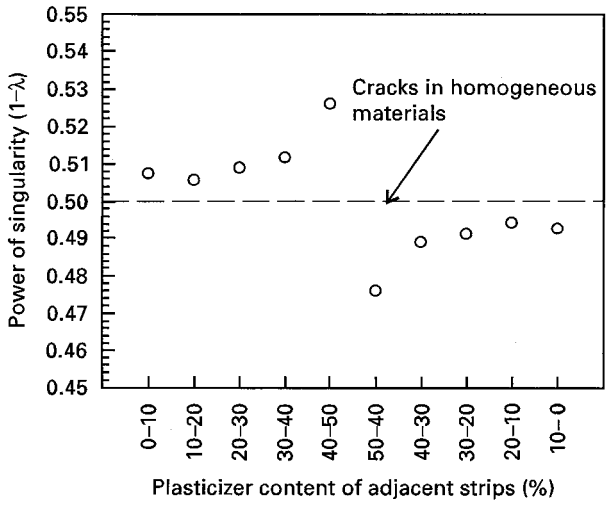

Figure 8 Variation of crack-tip singularity at the interface between strips having different properties (i.e. plasticizer content).

fringe constant. The stress field equations, when coupled with the stress-optic law (Equation 2), provide the relation that defines the isochromatic fringes around the moving crack tip. The isochromatic fringe patterns were analysed, and the coefficients of the series were obtained using the multi-point least squares method developed by Sanford and Dally [7].

4. Results and discussion

4.1. Crack velocity

The normalized crack length as a function of time for the various FGMs considered in this study is shown in Fig. 9. As can be seen from the figure, the crack propagated at constant velocity during the initial stages in all the FGMs. Fig. 9a shows the normalized crack length as a function of time for the 0–50 (increasing toughness) and 50–0 (decreasing toughness) FGMs. The ratio of the initiation toughness to the static toughness of the first strip containing the starter notch was held constant in these two experiments. The maximum velocity observed for the 0–50 FGM was $260\,m\,s^{-1}$ whereas for the 50–0 FGM, it was $320\,m\,s^{-1}$. It can be observed from Fig. 9a that the crack gradually decelerated before the final arrest in the 50–0 FGM. In the case of the 0–50 FGM, the crack arrested in a rather abrupt manner at the interface between 20% and 30% strips. It should be noted at this point that even though the ratio K_Q/K_{IC} was the same in these experiments, the K_Q value for the 50–0 FGM was 1.6 times that of the 0–50 FGM as the starter notch in the former case was in the 50% strip which has a higher toughness. Also, the corresponding energy in the specimen was almost 3 times larger for the 50–0 FGM as compared to the 0–50 FGM. These two factors together resulted in a larger crack velocity for the 50–0 FGM.

The normalized crack tip location history for the 0–50 (increasing toughness) and the 0–50–0 (increasing-decreasing toughness) FGMs are shown in Fig. 9b. In this set of experiments, the initial strain energy and the initiation stress intensity factor were held constant. It is clear from Fig. 9b that the curves

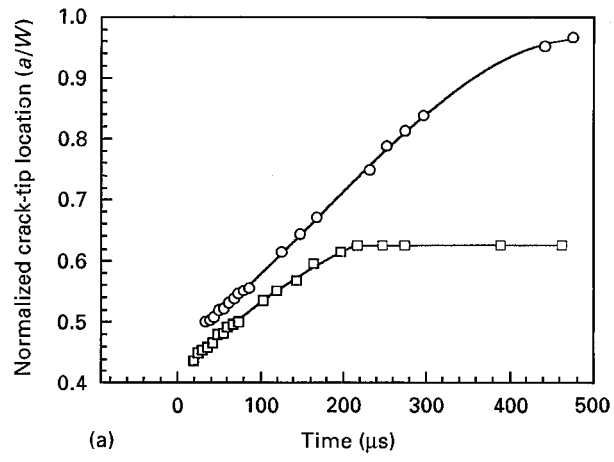

Figure 9a Crack-tip location history for the 0–50 (increasing toughness) (□, $K_{IC} = 0.51$ MPa $m^{1/2}$) and 50–0 (decreasing toughness) (○, $K_{IC} = 0.80$ MPa $m^{1/2}$) FGMs for the same ratio of $K_Q/K_{IC} = 1.6$ (K_{IC} – toughness of the first strip).

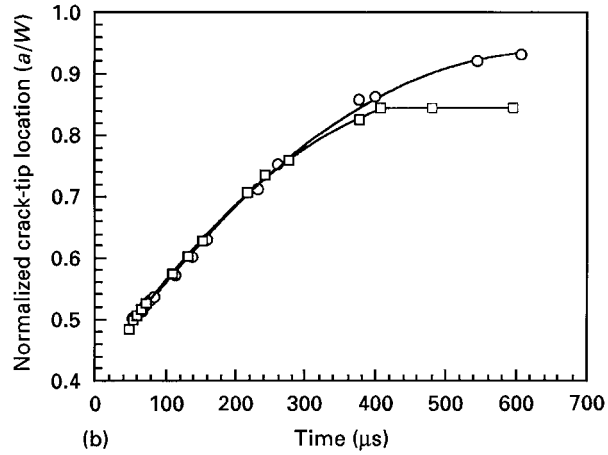

Figure 9b Crack-tip location history for the 0–50 (increasing toughness) (□) and 0–50–0 (increasing-decreasing toughness) (○) FGMs for the same initial energy and initiation stress intensity factor.

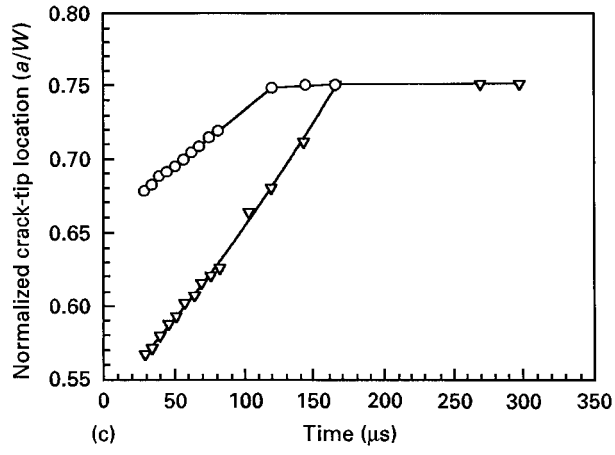

Figure 9c Crack-tip location history for the 0–50 (increasing toughness) (○) and 0–50–0 (decreasing-decreasing toughness) (▽) FGMs for the same initial energy and initiation stress intensity factor.

are very close to each other during the initial half of the crack propagation indicating that the velocity histories are similar, and the maximum observed velocities were 320 m s^{-1} and 300 m s^{-1}, respectively. In both these experiments, the crack velocity decreased gradually before the final arrest, and it can be seen from Fig. 9b that the crack propagated a greater distance in the case of the 0–50–0 FGM when compared to the 0–50 FGM.

Fig. 9c shows the crack-tip location history for the 50–0 (decreasing toughness) and the 50–0–50 (decreasing-increasing toughness) FGMs for the same initial energy and K_Q. In both these FGMs, the crack arrested at an interface after propagating through the same distance.

Previous studies on crack propagation across bimaterial interfaces by Dally and Kobayashi [8], and Theocaris and Milos [9] have shown arrest of the crack at the interface, followed by reinitiation. In the experiments conducted by Dally and Kobayashi [8], the two material halves were joined using a tough adhesive, and the time delay between arrest and reinitiation was of the order of 68 to 128 μs. In the experiments conducted by Theocaris and Milos [9], the bimaterial was prepared by casting one material over the other, and the time delay between arrest and reinitiation was 5 to 50 μs. In the present study, however, such a phenomenon was not observed explicitly. The plot of crack-tip location against time in Fig. 9 does not show any discernible discontinuities either.

4.2. Crack surface features

The fracture surface was examined under a Nikon Metaphot optical microscope to study the surface features. Particular attention was given to the region around the interfaces. Typical surface feature observed at an interface are shown in Fig. 10. Microscopic examination revealed that the interfaces were about 125 μm thick. Dense broom-stick marks were observed within the interface and also to a certain extent into the adjacent strip in the direction of crack propagation. These broomstick marks coalesced and became fewer as the crack propagated. On approaching the next interface, the broom-stick marks terminated at the first boundary of the interface, except for a few which were continuous across this boundary. These marks increased in number at the first boundary of the interface and traversed across the interface into the following strip in a continuous manner. These broom-stick marks indicate that higher energy is involved in driving the crack. Due to the high energy at the crack tip, the crack tries to branch into adjacent parallel planes leading to a non-planar crack front. This results in the formation of ridges in the fracture surface which appear as broom-stick marks [10].

In a homogeneous material, the crack surface appears rough with dense broom-stick marks near the initiation point and the surface becomes progressively smoother with the broom-stick marks becoming fewer in number for a decreasing K_D geometry, like the MCT. The surface features observed for the FGMs

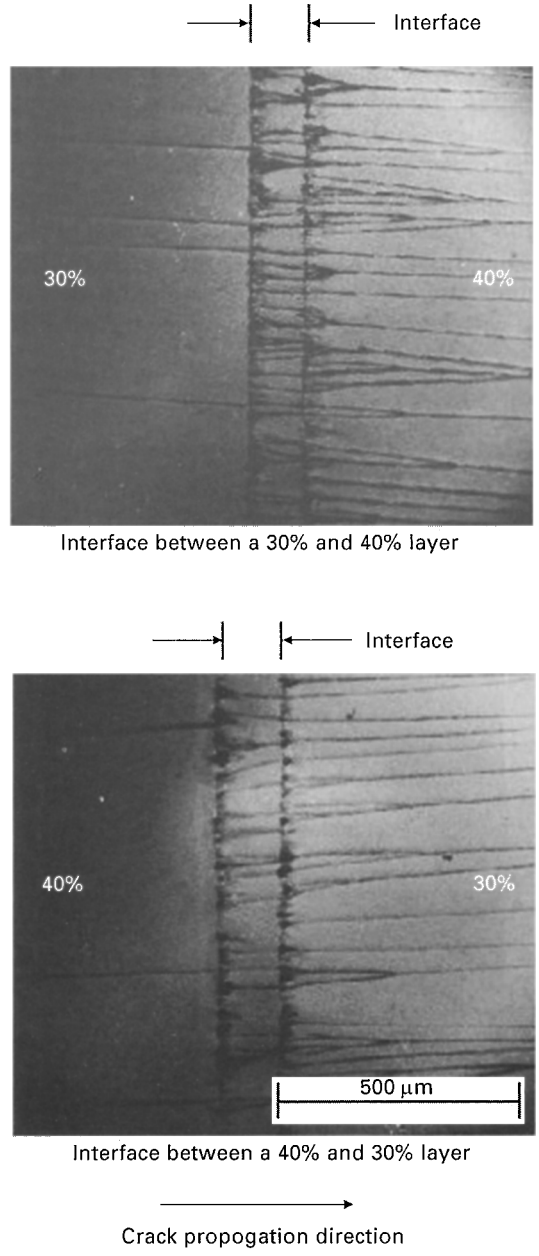

Figure 10 Fracture surface features near an interface.

were markedly different from this pattern, as explained above. The increased number of the broom-stick marks around the interfaces suggest that the microprocesses occurring at the interfaces are different from those in the adjacent homogeneous layers. The interfaces are potential sites for defects and voids which can act as crack initiation sites ahead of the propagating crack front. The crack front, on approaching the interface, interacts with the voids and defects that are present at the interface. This results in breaking of the crack front into several cracks propagating in adjacent parallel planes. After crossing the interface, these cracks regroup and become more planar in nature, resulting in a fewer number of broom-stick marks. These marks terminate and the surface becomes mirror-like before crack arrest, irrespective of whether the arrest occurs within the strips or at the interface.

4.3. Dynamic stress intensity factor

Typical isochromatic fringe patterns obtained for the 0–50–0 FGM are shown in Fig. 11. The dynamic stress intensity factor was evaluated from these isochromatic fringe patterns using the analysis procedure discussed in the previous section. The variation of dynamic stress intensity factor (K_D) for the 0–50 (increasing toughness) and 50–0 (decreasing toughness) FGMs for the same ratio of K_Q/K_{IC} is shown in Fig. 12a. The dynamic stress intensity factor showed a decreasing trend with increasing crack length for the 0–50 FGM. This is similar to the trend observed in homogeneous materials for the MCT geometry. After the crack arrest at the interface, the dynamic stress intensity exhibited an oscillatory behaviour. However, the K_D in the case of the 50–0 FGM remained constant for a short duration after initiation before decreasing monotonically, as can be observed from Fig. 12a.

The dynamic stress intensity factor for the 0–50 and the 0–50–0 FGMs exhibited an oscillatory behaviour as shown in Fig. 12b. The oscillatory behaviour is more prominent for the 0–50–0 FGM when compared to the 0–50 FGM. The presence of interfaces

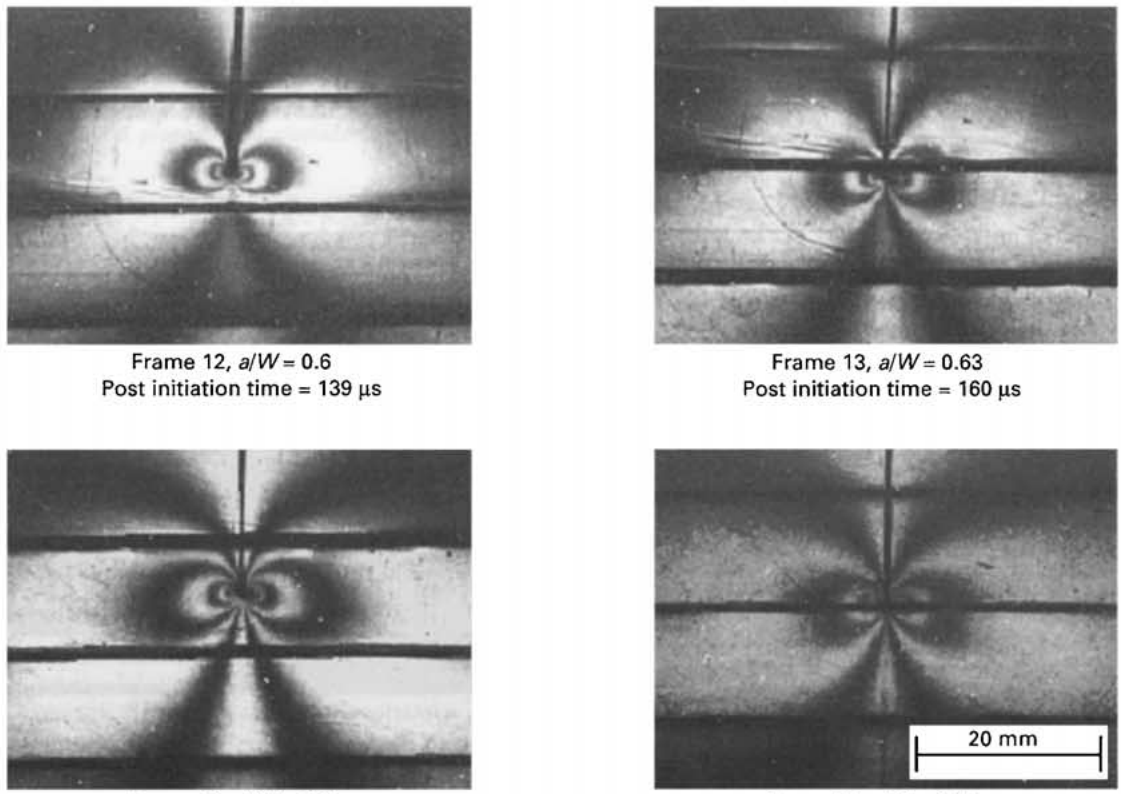

Figure 11 Typical isochromatic fringe patterns for a crack propagating in the 0–50–0 FGM.

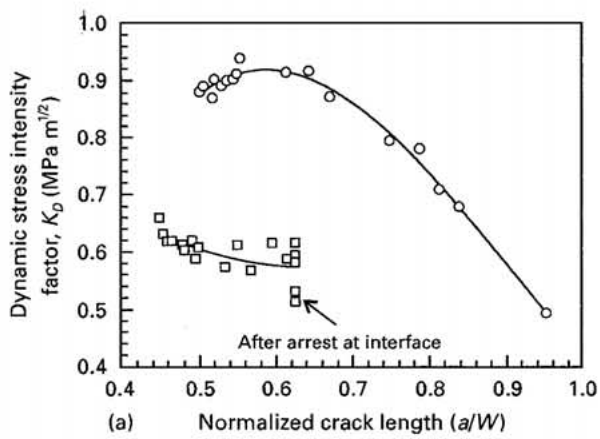

Figure 12a Dynamic stress intensity factor history for the 0–50 (increasing toughness) (□) and 50–0 (decreasing toughness) (○) FGMs for the same ratio $K_Q/K_{IC} = 1.6$ (K_{IC} – toughness of the first strip).

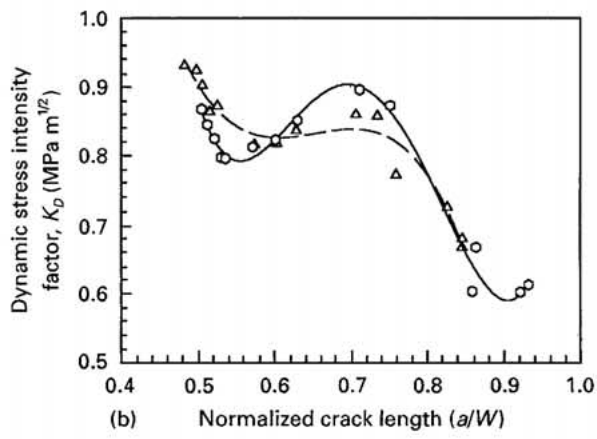

Figure 12b Dynamic stress intensity factor history for the 0–50 (increasing toughness) (– – – △) and 0–50–0 (increasing-decreasing toughness) (—○) FGMs for the same initial energy and initiation stress intensity factor.

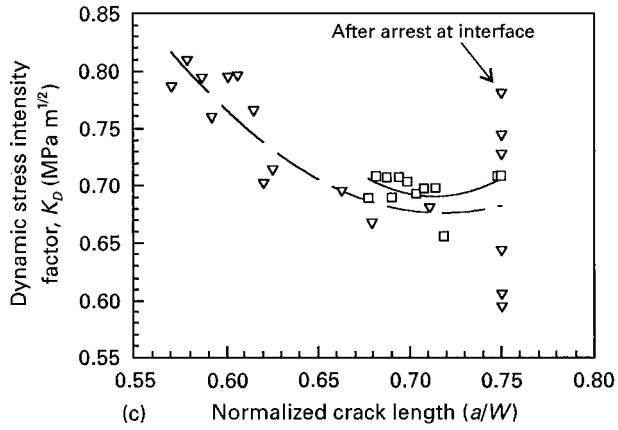

Figure 12c Dynamic stress intensity factor history for the 50–0 (decreasing toughness) (— □) and 50–0–50 (decreasing-increasing toughness) (– – ▽) FGMs for same initial energy and initiation stress intensity factor.

leads to reflections of the crack tip generated stress waves when compared to a monolithic specimen. These waves reaching the crack tip give rise to the oscillatory behaviour of the dynamic stress intensity factor.

In the case of the 50–0 (decreasing toughness) and 50–0–50 (decreasing-increasing toughness) FGMs, the dynamic stress intensity factor registered a monotonic decrease with increasing crack length, as shown in Fig. 12c. However, in these two FGMs, the crack arrested at the interface, and the dynamic stress intensity factor showed an oscillatory behaviour after crack arrest.

4.4. Crack jump distance

The crack jump distances obtained for the four different FGMs are summarized in Table III. It can be observed that, for the same ratio of K_Q/K_{IC}, the crack jump distance for the 50–0 FGM is 140% more than that obtained for the 0–50 FGM. It is clear from Table III that the initial energy for the 50–0 FGM was three times that of the 0–50 FGM. In addition, the toughness in the 50–0 FGM decreases in the direction of crack propagation, offering less resistance to crack propagation. These factors together resulted in a larger crack jump distance for the 50–0 FGM when compared to the 0–50 FGM.

The 0–50 and 0–50–0 FGMs were tested for the same value of initial energy and K_Q. The crack jump distance obtained for the 0–50–0 FGM is 20% more than that of the 0–50 FGM. This behaviour is due to the fact that in the 0–50–0 FGM, the toughness increases and then decreases in the direction of crack growth, whereas in the 0–50 FGM, the toughness increases. The overall resistance to crack propagation is less for the 0–50–0 FGM when compared to the 0–50 FGM, and this caused the increase in crack jump distance. In the 50–0 and 50–0–50 FGMs, which were tested under the same initial energy and K_Q, the crack arrested at the interface after propagating through the first five strips.

5. Conclusions

A material system consisting of polyester resin and plasticizer to be used for preparing functionally gradient materials suitable for photoelastic studies was identified, and the properties of the material were evaluated for different compositions. An FGM with discrete property variation was prepared, and dynamic crack propagation in this FGM was studied. The results of this study indicate the following:

- Increasing the plasticizer content from 0% to 50% resulted in a 45% decrease in the Young's modulus, whereas the fracture toughness increased by 60%.
- The material fringe constant remained insensitive to plasticizer content.
- The dynamic properties of the material exhibited no variation with increasing plasticizer content. However, the rate sensitivity of the material increased by 80% as the plasticizer content was increased from 0% to 50%.
- Results of dynamic fracture studies for different property variations showed that increasing the toughness in the direction of crack propagation results in smaller crack jump distances as compared to increasing-decreasing toughness in the direction of crack propagation for the same initial energy.
- The dynamic stress intensity factor exhibited an oscillatory behaviour for the increasing toughness and increasing-decreasing toughness FGMs before the crack arrest, whereas, it decreased monotonically in the decreasing toughness and decreasing-increasing toughness FGMs.

Acknowledgements

The support of the National Science Foundation under grant number CMS 9424114 is gratefully acknowledged. The authors also acknowledge Ashland Chemical Company for providing the resins used in this study.

References

1. F. ERDOGAN, *Compos. Eng.* **5** (1995) 753.
2. R. C. BATRA and Z.-H. JIN, *J. Mech. Phys. Solids* **44** (1996) 1221.
3. J. W. DALLY and W. F. RILEY, "Experimental Stress Analysis", 3rd Edn (McGraw-Hill Publications, New York, 1991).
4. H. KOLSKY, "Stress Waves in Solids", 2nd Edn (Dover Publications, New York, 1963).
5. G. R. IRWIN, University of Maryland Lecture Notes (1980).
6. T. S. COOK and F. ERDOGAN, *Int. J. Eng. Sci.* **10** (1972) 677.
7. R. J. SANFORD and J. W. DALLY, *Eng. Fract. Mech.* **11** (1979) 621.
8. J. W. DALLY and T. KOBAYASHI, *Int. J. Solids Struct.* **14** (1978) 121.
9. P. S. THEOCARIS and J. MILOS, *Int. J. Fract.* **16** (1980) 31.
10. A. C. ROULIN-MOLONEY, "Fractography and Failure Mechanisms of Polymers and Composites" (Elsevier Science Publishers, New York, 1988).

Received 19 May 1997
and accepted 7 April 1998